Integrated modelling of the ramp-up phase of JT-60SA baseline and hybrid scenarios in view of operations

S. Gabriellini[1], L. Garzotti[2], V. K. Zotta[1], J.F. Artaud[3], R. Gatto[1], G. Giruzzi[3], C. Sozzi[4] , D. Taylor[2], T. Wakatsuki[5], and the JT-60SA Integrated Project Team
[1]*Dipartimento di Ingegneria Astronautica, Elettrica ed Energetica, Sapienza Università di Roma, via Eudossiana 18, 00184, Roma, Italy*
[2]*United Kingdom Atomic Energy Authority, Culham Science Centre, Abingdon, Oxon, OX14 3DB, United Kingdom of Great Britain and Northern Ireland*
[3]*CEA, IRFM, F-13108 Saint Paul Lez Durance, France*
[4]*ISTP Istituto di Scienza e Tecnologia del Plasma – CNR, Milano, Italy*
[5]*National Institutes for Quantum Science and Technology, Naka 311-0193, Japan*

1. Introduction The JT-60SA superconducting tokamak, built and operated jointly by Europe and Japan, achieved its first plasma in October 2023. This will be the largest magnetically confined fusion experiment in the world for the coming years, before the start of ITER operations, supporting the exploitation of ITER and the investigation of key physics and engineering issues for future demonstration power plants [1, 2]. The parameters of the scenarios that will be studied by JT-60SA, reported in [1, p. 10], have been determined with the help of the equilibrium code ACCOME, then checked and improved with 0.5-D simulations using the METIS code [3] and finally confirmed by means of more sophisticated 1.5-D transport codes [4]. The ramp-up phase of the advanced inductive (hybrid) scenario has also been modelled with the JINTRAC [5] suite of codes, confirming the results of METIS [6], and with the CRONOS code [7]. However, the scenarios that will be developed in the next operational phase (**OP2**), expected to start in ~2026, will be limited by the heating and current drive availability of the machine, as well as by the heat handling capability of the first lower divertor, and will therefore differ from the target scenarios. Consequently, a great effort is being devoted to the initial development of integrated scenarios, including transport predictions, MHD stability and control, in order to maximise the scientific outcome of the Initial Research Phase within the capabilities of the machine. This work shows the results of the predictive integrated modelling of the baseline and hybrid scenarios in view of OP2, whose global parameters are reported in Table 1. The scenarios reported here are meant as a starting point for future optimizations and a first step for approaching their maximum parameters.

	OP2 Hybrid	OP2 Baseline
Species	D	D
B_t $[T]$	1.7	2.28
I_p $[MA]$	2.7	4.6
f_{bs} [%]	34.6	13.9
f_{ni} [%]	68.9	32.6
f_{gw} [%]	60.5	41.9
q_{95}	4.6	3.6
P_{nbi} $[MW]$	15.7	15.7
P_{ecrh} $[MW]$	1.5 + 1.5	1.5
$n_{e,0}$ $[10^{19}m^{-3}]$	4.7	5.2
$< n_e >$ $[10^{19}m^{-3}]$	4.0	4.4
$T_{e,0}$ $[keV]$	6.3	6.5
$< T_e >$ $[keV]$	3.2	3.2
$T_{i,0}$ $[keV]$	6.6	7.1
$< T_i >$ $[keV]$	3.0	3.0
W_{th} $[MJ]$	6.8	8.2
H_{98}	1.3	0.9
β_N, β_p	3.0, 1.2	1.5, 0.4
τ_E $[s]$	0.3	0.6
Z_{eff}	2.1	1.8
$neutrons$ $[10^{16}s^{-1}]$	3.8	4.1

***Table 1** – Main plasma parameters computed by JINTRAC for the OP2 hybrid and OP2 baseline scenarios, averaged in the flat-top phase.*

2. Description of the simulations The predictive integrated modelling has been performed with the JINTRAC suite of codes [5], starting from the ramp-up phase up to a few seconds into the flat-top, using JETTO [8] as 1.5-D transport code, coupled with the semi-empirical Bohm/gyro-Bohm transport model (BgB) [9]. We are predicting the main ion density (Deuterium), electron and ion temperatures and current density. The predictive capability of BgB has been tested on JET and JT-60U scenarios similar to the one foreseen for JT-60SA, showing that it can provide a

good first estimate of the temperatures, typically slightly overestimating them [10]. Moreover, the integrated modelling framework used in this work is being validated against pulses that were recently performed at JET with dimensionless parameters (ρ^*, ν^*, β_N) most similar to the ones of JT-60SA scenarios [11], and first results are showing a good agreement with the experimental kinetic profiles. The starting point of the modelling of the OP2 hybrid scenario is a METIS simulation of the high-power version, which we scaled down to comply with the machine capabilities, whereas for the OP2 baseline scenario a METIS simulation of the low-power version is used as reference. We impose the same waveforms of the plasma current (I_p), line-averaged electron density ($< n_e >$), Neutral Beam Injection (P_{nbi}) and Electron Cyclotron Resonance Heating (P_{ecrh}), as well as the evolution in time of the plasma boundary as METIS. The latter has been evaluated by METIS coupled with the free boundary equilibrium solver FEEQS, which allows to check the feasibility of the scenario in terms of currents, voltages and forces in the poloidal field coils [12]. In order to follow the prescribed $< n_e >$ ramp, a feedback loop acting on the gas puff is used in FRANTIC [13]. The boundary conditions are imposed at the separatrix, where the temperatures are $T_e = T_i = 100\ eV$ and the ion density is evolved in time to follow the METIS value. The equilibrium is computed with the fixed-boundary code ESCO [14], self-consistently with the evolution of the kinetic profiles. In order to compute the NBI and ECRH heating deposition and current drive, the codes PENCIL [15] and GRAY [16] are used respectively. The impurity considered is Carbon, for which we prescribed radially constant Z_{eff} and P_{rad} profiles, not evolving the transport at this stage of the modelling. The L-H transition is predicted consistently with the use of Martin scaling [17]. The transport within the Edge Transport Barrier (ETB) is modelled in the H-mode phase with the empirical Continuous ELM model [18], where the normalised critical pressure gradient α_c is kept constant by artificially increasing the transport coefficients in that region. The values of the α_c for the two scenarios are being verified through linear MHD stability analysis using the MISHKA [19] code, and first results are confirming the chosen values of 1.6 (hybrid) and 1.0 (baseline), although further investigations are needed.

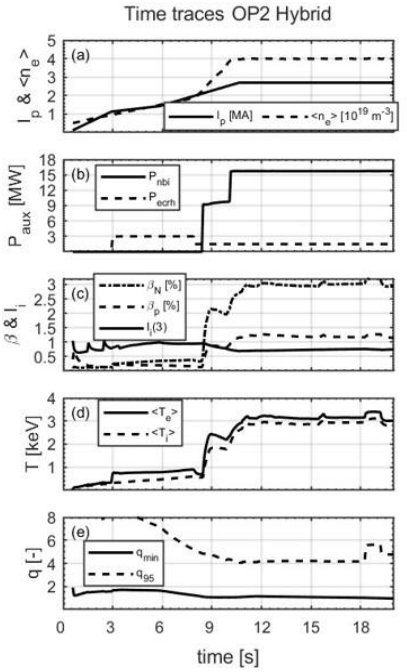

Figure 1 *– Time traces of Scenario 4.2. From top to bottom: plasma current and averaged electron density, NBI and ECRH power, β_N, β_p and $l_i(3)$, ion and electron averaged temperatures, minimum and 95% flux surface safety factor.*

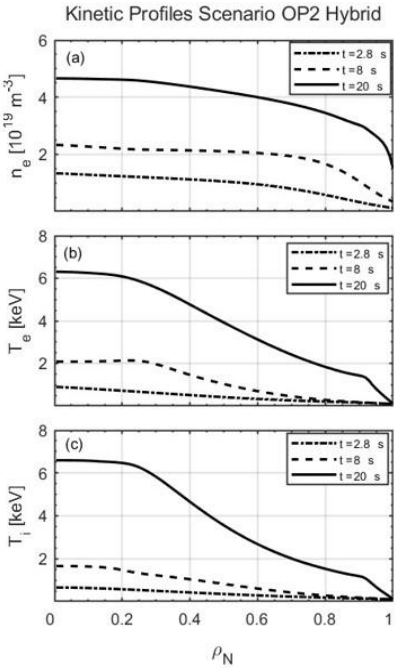

Figure 2 *– Kinetic profiles of Scenario 4.2. From top to bottom: electron density, electron temperature and ion temperature at three different times, plotted against the normalised toroidal flux coordinate ρ_N.*

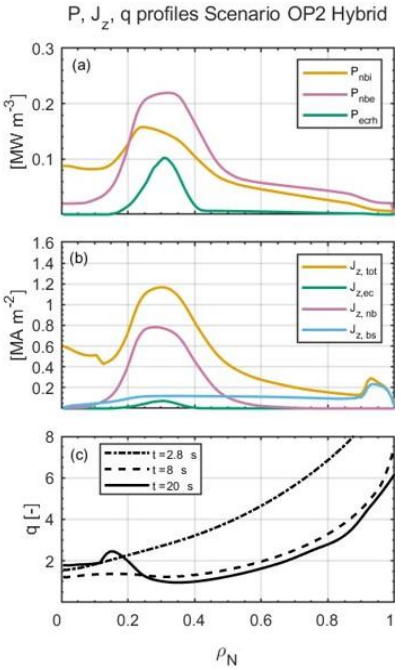

Figure 3 *– Profiles of the power deposition, current density and safety factor for Scenario 4.2. The power and current densities are averaged in the flat-top phase, while the safety factor is plotted at three different times.*

3. OP2 Hybrid scenario The first modelled scenario is a H-mode, high β_N scenario, with $I_p = 2.7\ MA$, $B_t = 1.7\ T$, q_{95}~4.6, β_N~3.0. The main parameters of the scenarios are summarized in the left column of Table 1. The auxiliary heating is provided by the Electron Cyclotron Resonance Heating (ECRH) for a total power of 3 MW and by the Neutral Beam Injection (NBI) for a total power of 16 MW. Regarding the ECRH, 1.5 MW are provided steadily by two gyrotrons with steerable launchers at 110 GHz in X-mode, while the other 1.5 MW are supplied only for 5 seconds by the other two gyrotrons without steerable launchers at 110 GHz in X-mode. The frequency is chosen so to have absorption at the 2nd harmonic with the given magnetic field of 1.7 T, whereas the location of the deposition at ρ~0.3 is chosen following the results shown in [7]. Concerning the NBI, this is divided into 10 MW of Negative-NBI, with two units (upper and lower) with beams at 500 keV which drive a strong off-axis current, and 6 MW of Positive-NBI, with beams at 85 keV. The evolution in time of the main plasma parameters is presented in Figure 1, whereas the profiles of the electron density (n_e), electron temperature (T_e) and ion temperature (T_i) plotted against the normalised toroidal flux coordinate ρ_N are presented in Figure 2. The latter are plotted at three different times: 2.8 seconds (just before the start of ECRH), 8 seconds (just before the start of NNBI and the entrance in H-mode) and 20 seconds (~9 seconds into the flat-top phase). The Bohm/gyro-Bohm transport model is predicting values of the on-axis temperatures equal to $T_{e,0} \sim 6.3\ keV$ and $T_{i,0} \sim 6.6\ keV$, with flat profiles from $0 < \rho_N < 0.2$, where the model is finding low turbulence levels. As a consequence the bootstrap current contribution is decreasing in that region, as clear from Fig.3-(b). The tailoring of the current profile in order to maintain the safety factor profile above one and avoiding sawtooth activity is one of the goals of the hybrid scenario. In the ramp-up phase, the 3 MW of ECRH for 5 seconds are providing a strong heating of the electrons that in turn is helping slowing down the current diffusion and keeping the q profile above one. In fact, to test the relevance of ECRH in the ramp-up phase, we ran a simulation without ECRH, predicting a $q = 1$ arrival time of 4.3 s. As can be seen from Fig. 3-(c), the q profile just before the entrance in H-mode (~8 s) is flat in the core and above one for the

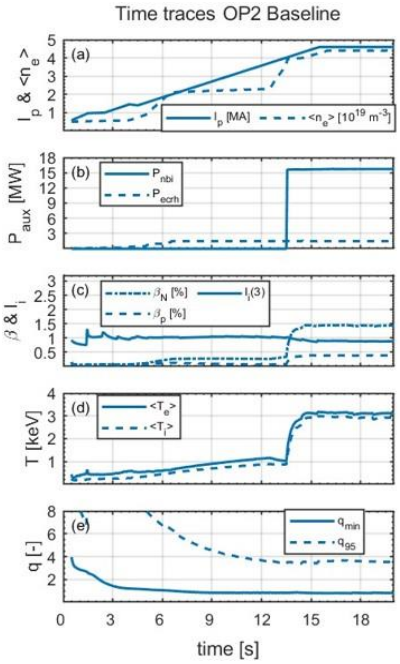

Figure 4 *- Time traces of the OP2 baseline scenario. From top to bottom: plasma current and averaged electron density, NBI and ECRH power, β_N, β_p and $l_i(3)$, ion and electron averaged temperatures, minimum and 95% flux surface safety factor.*

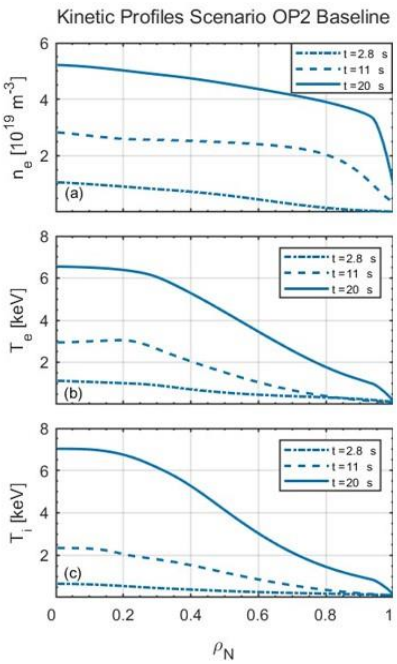

Figure 5 *– Kinetic profiles of the OP2 baseline scenario. From top to bottom: electron density, electron temperature and ion temperature at three different times, plotted against the normalised toroidal flux coordinate ρ_N.*

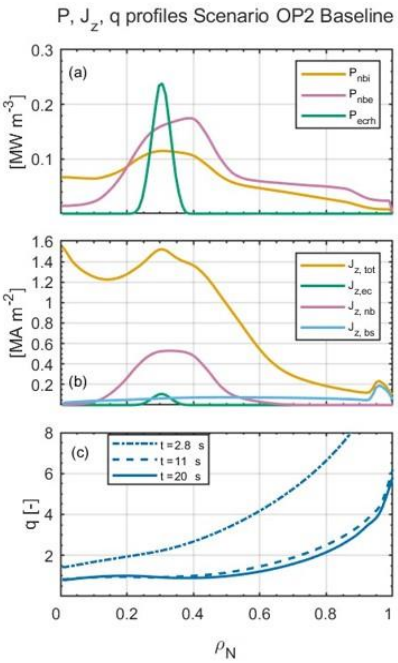

Figure 6 *– Profiles of the power deposition, current density and safety factor of the OP2 baseline scenario.. The power and current densities are averaged in the flat-top phase, while the safety factor is plotted at three different times.*

whole plasma radius. However, when the NBI is switched on, a strong off-axis current is driven, clearly visible from Fig. 3-(b), which is leading to a slightly reversed q profile at the end of the flat-top phase. The clamping of the q profile between $0 < \rho_N < 0.1$ to a value of 1.9 is needed due to the numerical difficulties encountered by ESCO in computing the equilibrium with hollow current profiles.

4. OP2 Baseline scenario The second modelled scenario is a H-mode, high current and high field scenario, with $I_p = 4.6\ MA, B_t = 2.28\ T, q_{95}$~3.6, β_N~1.5. The main parameters of the scenarios are summarized in the right column of Table 1. The auxiliary heating is very similar to the one of the hybrid scenario, with the only difference being the total ECRH power and frequency used. In fact, 1.5 MW of ECRH are injected for the whole duration of the simulation at a frequency of 138 GHz in X-mode, in order to have the absorption at the 2nd harmonic. The strong electron heating during the ramp-up phase is not as necessary in this scenario as it is in the hybrid, and the sawtooth activity that is generated by a relaxed current profile will be investigated in the Initial Research Phase, in view of future ITER baseline operations. To model the sawtooth activity, the Kadomstev model [20] is used, where the period of the sawtooth is prescribed and equal to 200 ms. The $q = 1$ arrival time is predicted to be around $t_{q=1} \sim 6.3\ s$. The time traces of the JINTRAC simulation are shown in Fig. 4, while the profiles of n_e, T_e *and* T_i are shown in Fig. 5. The BgB transport model, similarly to the hybrid scenario, is predicting low turbulence levels between $0 < \rho_N < 0.2$, but with higher on-axis temperatures, despite a lower temperature pedestal and lower ECRH power. This is due to the higher confinement at higher current and field achieved in the baseline, where τ_E~0.6 s in the flat-top phase which is double than the one of hybrid. In both scenarios we are well above the L-H threshold computed by Martin scaling (P_{LH}~ 8 MW for the baseline and 5 MW for the hybrid).

5. Future work Two scenarios, baseline and hybrid, were modelled with JINTRAC in view of JT-60SA next operational phase (OP2). Future work will focus on: (i) checking the controllability of the scenario by iterating JINTRAC simulation with an equilibrium control code, e.g. CREATE-NL (ii) extending the modelling to the ramp-down phase, (iii) starting to model the transport of impurities with SANCO, (iv) using CDBM and first-principle transport models, e.g. QuaLiKiz and TGLF, (v) improving the NBI predictions with the Monte Carlo code ASCOT, (vi) possibly using the same modelling framework for predicting other JT-60SA scenarios.

Acknowledgements

This work has been carried out within the framework of the EUROfusion Consortium, funded by the European Union via the Euratom Research and Training Programme (Grant Agreement No 101052200 — EUROfusion). Views and opinions expressed are however those of the author(s) only and do not necessarily reflect those of the European Union or the European Commission. Neither the European Union nor the European Commission can be held responsible for them.

JT-60SA was jointly constructed and is jointly funded and exploited under the Broader Approach Agreement between Japan and EURATOM.

References

[1] JT-60SA Research Plan, version 4.0 (September 2018)
[2] G Giruzzi et al 2020 Plasma Phys. Control. Fusion 62 014009.
[3] G. Giruzzi et al, 2012, 39th EPS Conference & 16th Int. Congress on Plasma Physics (P5.018).
[4] Garzotti L. et al 2018 Nucl. Fusion 58 026029.
[5] Romanelli M. et al 2014 Plasma and Fusion Research 9 3403023.
[6] S. Gabriellini et al, 2023, 49th EPS Conference on Contr. Fusion and Plasma Phys, 3-7 July (P1.062).
[7] J Morales et al 2021 Plasma Phys. Control. Fusion 63 025014
[8] Cenacchi G. and Taroni A. 1988 JETTO: a free-boundary plasma transport code Rapporto ENEA RT/TIB/88/5.
[9] Erba M. et al 1997 Plasma Phys. Control. Fusion 39 261.
[10] Garcia J. et al 2014 Nucl. Fusion 54 093010.
[11] Orsitto et al, this conference.
[12] V. Ostuni et al 2021 Nucl. Fusion 61 026021
[13] Tamor S. 1981 J. Comput. Phys. 40 104.
[14] Cenacchi G. and Rulli M. 1988 Upgrading of an equilibrium transport code for a multispecies free-boundary plasma ENEA Report RTI/TIB(88)5.
[15] Challis C.D. et al 1989 Nucl. Fusion 29 563.
[16] Farina D. 2007 Fus. Sc. Tec., 52:2, 154-160.
[17] Martin Y.R. et al 2008 J. Phys.: Conf. Ser. 123 012033.
[18] Parail V. et al 2009 Nucl. Fusion 49 075030.
[19] Mihailovskii A.B. et al 1997 Plasma Phys. Rep. 23 844.
[20] Kadomstev B.B. 1975 Sov. J. Plasma Phys. 1 389